Early Holocene ice retreat from Isle Royale in the Laurentian Great Lakes constrained with [10]Be exposure-age dating

Eric W. Portenga[1], David J. Ullman[2], Lee B. Corbett[3], Paul R. Bierman[3], Marc Caffee[4]

[1] Geography and Geology Department, Eastern Michigan University, Ypsilanti, MI 48197
5 [2] Geology Department, Northland College, Ashland, WI 54806
[3] Rubenstein School of Natural Resources and the Environment, University of Vermont, Burlington, VT 05405
[4] PRIME Laboratory, Purdue University, West Lafayette, IN 47907

Correspondence to: Eric W. Portenga (eric.portenga@emich.edu)

Abstract. The timing of the Laurentide Ice Sheet's final retreat from North America's Laurentian Great Lakes is relevant to
10 understanding regional meltwater routing, changing proglacial lake levels, and lake-bottom stratigraphy following the Last
Glacial Maximum. Recessional moraines on Isle Royale, the largest island in Lake Superior, have been mapped but not
previously dated. Here, we use the mean of ten new [10]Be exposure-ages of glacial erratics from two recessional moraines
(10.1 ± 1.1 ka, one standard deviation; excluding one anomalously young sample) to constrain the timing of Isle Royale's
final deglaciation. This [10]Be age is consistent with existing minimum limiting ^{14}C ages of basal organic sediment from two
15 inland lakes on Isle Royale, a sediment core in Lake Superior southwest of the island, and an estimated deglaciation age of
the younger of two subaqueous moraines between Isle Royale and Michigan's Keweenaw Peninsula. Relationships between
Isle Royale's landform ages and Lake Superior bottom stratigraphy allow us to delineate the retreat of the Laurentide ice
margin across and through Lake Superior in the early Holocene. We suggest Laurentide ice was in contact with the southern
shorelines of Lake Superior later than previously thought.

1 Introduction

Following the Last Glacial Maximum (LGM), the southwest margins of the Labrador Dome of the Laurentide Ice Sheet
(LIS) retreated, exposing the Laurentian Great Lakes of North America (hereafter referred to as the Great Lakes, Fig. 1).
Initial retreat of the LIS from LGM margins in the Great Lakes region is associated with increased summer boreal insolation
(Clark et al., 2009; Ullman et al., 2015). Ice retreat through the Great Lakes appears to have been mostly continuous across
25 the late-Pleistocene-Holocene transition (Lowell et al., 2021) with some clear exceptions of ice advance during the
Marquette Readvance of the Younger Dryas (Loope, 2006; Lowell et al., 1999, 2009). Meltwater from the LIS accounts for
~50–60% of the late-Pleistocene sea-level budget (Clark and Mix, 2002), so constraining spatial and temporal retreat
patterns of the LIS southwest margins through the Great Lakes improves understanding of meltwater routing from proglacial
lakes to the oceans (Broecker, 2006; Broecker et al., 1989; Carlson et al., 2007; Fisher, 2020; Leydet et al., 2018; Teller,

30   1990; Teller and Mahnic, 1988; Teller et al., 2002, 2005) and proglacial lake organization (Breckenridge, 2013; Farrand, 1969).
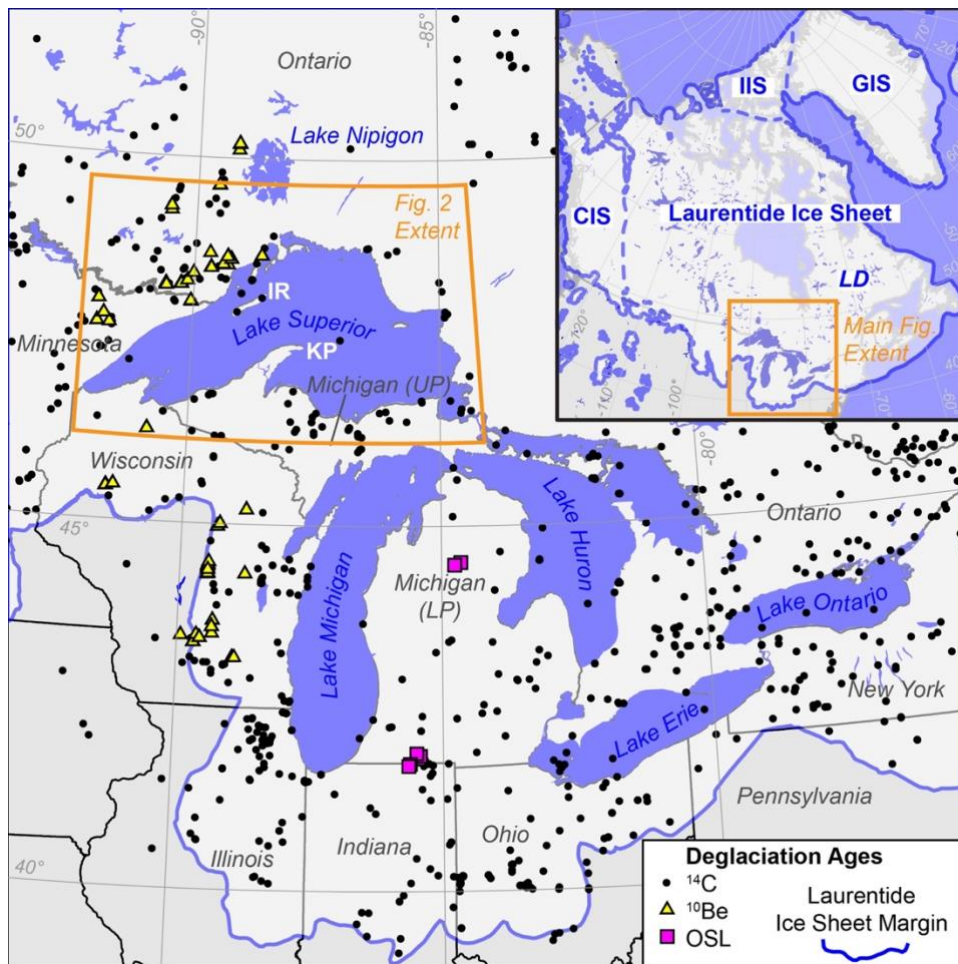
Figure 1. The Laurentian Great Lakes of North America and the Laurentide Ice Sheet (LIS) margins at the Last Glacial
35   Maximum (LGM; solid blue line; Ehlers et al., 2011). Inset figure shows full extent of the North American LGM ice cover inclusive of the Cordilleran (CIS), Greenland (GIS), Innuitian (IIS) Ice Sheets (Ehlers et al., 2011) and the Labrador Dome (LD) where ice that forms the Laurentide Ice Sheet's southwest margins originates. Existing sample sites for ^{14}C data (black dots; Dalton et al., 2020), [10]Be data (yellow triangles; Ceperley et al., 2019; Kelly et al., 2016; Leydet et al., 2018; Lowell et al., 2021; Ullman et al., 2015), and OSL (purple squares; Fisher et al., 2020; Schaetzl et al., 2017). Only US states and
40   Canadian provinces covered by the Laurentide Ice Sheet are shown; the state of Michigan comprises the lower peninsula (LP) and upper peninsula (UP). Locations of Isle Royale (IR) and Keweenaw Peninsula (KP) are shown.

Although previous work has investigated the age and rate of ice retreat through the Great Lakes region (Dalton et al., 2020;

Dyke, 2004), geochronological constraints on the timing of ice retreat are sparse, especially within lake basins, and Dalton et

45   al. (2020) note that the chronology of Laurentide Ice retreat through the Great Lakes has not received as much attention by

researchers as other margins of the LIS over the last twenty years. The existing chronology of ice retreat from the Great

Lakes is constrained primarily by minimum-limiting ^{14}C ages, most of which come from the southern LGM margins of the LIS (Dyke, 2004; Dalton et al., 2020; Fig. 1). Additional constraints on the timing of ice retreat from the Great Lakes region include [10]Be exposure age dating (Ceperley et al., 2019; Colgan et al., 2002; Leydet et al., 2018; Lowell et al., 2021; Ullman et al., 2015; Fig. 1) and in some cases, optically stimulated luminescence burial-age dating (e.g. Fisher et al., 2020; Schaetzl et al., 2017).

Lake Superior is the largest and northernmost of the Great Lakes and the largest freshwater lake by surface area in the world (IAGLR, 2012). Despite decades of geochronological efforts mapping ice margin positions across Lake Superior (e.g. Bajc et al., 1997; Black, 1976; Leydet et al., 2018; Lowell et al., 1999, 2005, 2009, 2021; Saarnisto, 1974), the long distances between shorelines and the paucity of dateable organic material retrieved from lake-bottom sediments has hampered development of a detailed history of LIS retreat across the lake (Breckenridge, 2007; Breckenridge et al., 2004; Hyodo and Longstaffe, 2011). Thus, uncertainties about LIS retreat across the lake following the LGM, and hence meltwater routing and proglacial lake organization, remain. For instance, advance of the Superior Lobe of the LIS to the Marks and the Grand Marais I moraines is well constrained to ~11.9 cal ka during the Marquette Readvance (Fig. 2; Loope, 2006; Lowell et al., 1999, 2009; all published ^{14}C ages cited in this study were rounded to the nearest 100 years and none are significantly different than those recalibrated using CALIB rev. 8, Stuiver et al., 1993), a brief period of ice growth during the Younger Dryas stadial (Carlson, 2010). However, it is unclear how far ice advanced in the western Lake Superior basin (Fig. 2; Black, 1976; Clayton and Moran, 1982; Colman et al., 2020; Drexler et al., 1983; Farrand and Drexler, 1985; Peterson, 1985). This uncertainty results from a lack of dateable material in Lake Superior sediments, the paucity of well-defined ice-marginal deposits associated with the Marquette Readvance around the western Lake Superior basin, and alternative interpretations for existing ^{14}C ages and stratigraphy (Colman et al., 2020; Hobbs and Breckenridge, 2011).

Recent geochronological work around Lake Superior focuses on retreat of the LIS's Superior Lobe along the northwest shore (the North Shore; Fig. 2) leading up to and following the Marquette Readvance, rather than establishing cross-lake relationships between the North Shore chronology and those of Wisconsin or Michigan's UP (Fig. 2). Along the North Shore, final retreat of the Superior Lobe uncovered eastward-draining outlets from Glacial Lake Agassiz to the Lake Superior basin via Lake Nipigon (Fig. 2; Fisher, 2020; Kelly et al., 2016; Leydet et al., 2018; Lowell et al., 2009, 2021; Teller and Mahnic, 1988). Meltwater flowed through western Lake Superior to eastern Lake Superior and drained through the Au Train-Whitefish Outlets to Lake Michigan and later through the St. Mary's River (Fig. 2; Breckenridge, 2013). However, the path meltwater took through Lake Superior during this drainage is unclear because ice margin positions remain less well-constrained since there is less recent research and dating in this area (Drexler, 1981; Huber, 1973; Hughes, 1963).
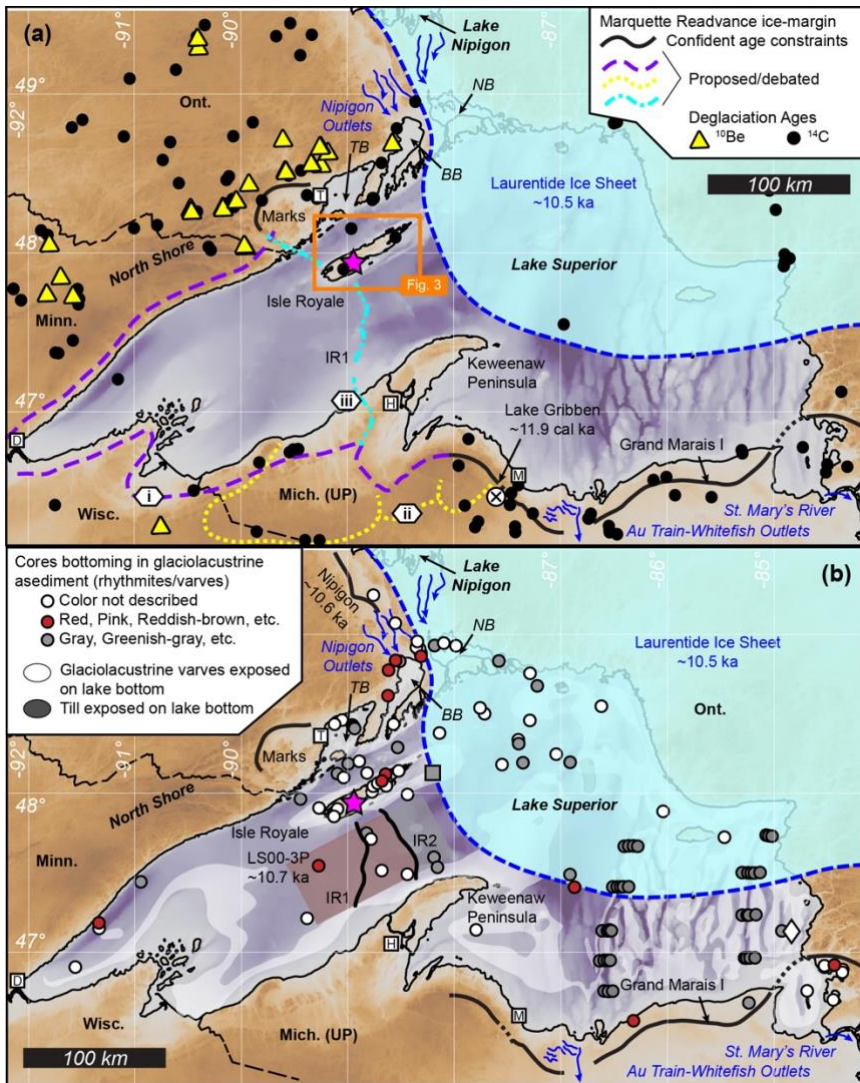
Figure 2. A. Lake Superior basin is shown with locations of moraines known to be associated with Younger Dryas ice advance: the Marquette Readvance (solid black lines). Ice margin positions thought to be associated with the Marquette Readvance: dashed purple line (<i>; Black, 1976; Clayton and Moran, 1982; Drexler et al., 1983; Hughes and Merry, 1978); stippled yellow line (<ii>; Peterson, 1985); cyan dash-dot line (<iii>; Colman et al., 2020). Black dots are existing ^{14}C data locations (Dalton et al., 2020); Yellow triangles are existing [10]Be locations (Leydet et al., 2018; Lowell et al., 2021; Ullman et al., 2015). The Lake Gribben forest bed site (Lowell et al., 1999), which constrains the timing of the Marquette Readvance and the Grand Marais I moraine complex, is specifically shown by a white circle with a black X. B. Lake Superior basin is shown with locations of cores where varves (red, gray, or no color reported) have been identified; the LS00-3P sediment core constrains ice-free conditions by ~10.7 ka (Breckenridge, 2007). The gray square northeast of Isle Royale in panel B is a shallow rise where gray varves directly overly till (Mothersill and Fung, 1972). The Laurentide Ice Sheet margin at ~10.5 ka in both panels is from Breckenridge (2013). The pink star in both panels is location of new [10]Be data presented here. Abbreviated locations of the Lake Superior basin mentioned in this study include Thunder Bay (TB), Black Bay (BB), and Nipigon Bay (NB); regional cities include Duluth (D), Houghton (H), Marquette (M), and Thunder Bay (T).

Here, we present eleven new [10]Be exposure ages of glacial erratics from the crests of recessional moraines on Isle Royale (Huber, 1973), the largest island in Lake Superior (Fig. 2). Isle Royale is proximal to and strikes parallel with the well-constrained North Shore deglaciation chronology (Fig. 2; Kelly et al., 2016; Leydet et al., 2018; Lowell et al., 2009, 2021). The island's position in the middle of Lake Superior offers a unique opportunity to extend the limits of the existing deglacial chronology and draw chronological relationships between the north and south shores of the Lake Superior basin and the lake bottom stratigraphy therein. We place our interpretation of new [10]Be ages in the context of the Lake Superior North Shore deglaciation chronology, two existing ^{14}C ages from inland lakes on Isle Royale (Flakne, 2003), and a dated lake-bottom sediment core southwest of Isle Royale (Breckenridge, 2007).

2 Study Location: Isle Royale and the Lake Superior Basin

Ice retreat across the western Lake Superior basin is constrained by only a handful of stratigraphic and chronological studies. For example, organic ^{14}C and [10]Be exposure ages of landforms along the northwest shore of Lake Superior demonstrate early and nearly-constant ice retreat to moraines at Lake Nipigon (north of Lake Superior) by ~10.6 ka where outlets from Glacial Lake Agassiz were opened to the Lake Superior basin at Black Bay (Fig. 2a; Leydet et al., 2018; Lowell et al., 2009, 2021; Teller and Mahnic, 1988). Both red and grey varves are present on the bottom of Lake Superior. Red varves are stratigraphically older and sourced from red clay, till, and bedrock in the southwest Lake Superior region, compared to the younger gray varves, which are sourced from the bedrock of the Canadian Shield (Breckenridge et al., 2021; Farrand, 1969). Lake Agassiz drainage into the Lake Superior basin is associated with the onset of red varve deposition in areas that were ice-free at the time (Fig. 2b; Breckenridge and Johnson, 2009), most likely when lake levels were between Duluth and Minong stages (Breckenridge, 2004; Colman et al., 2020; Teller and Mahnic, 1988). In the western Lake Superior basin, red varves are identified north of Isle Royale, in some inland lakes on Isle Royale's northern margin (Figs. 2b, 3a), and down-ice of the IR2 moraine (Fig. 2b; Breckenridge, 2007; Breckenridge et al., 2004; Colman et al., 2020; Maher, 1977; Raymond et al., 1975; Teller and Mahnic, 1988).

Red varves are also observed in parts of the eastern Lake Superior basin (Fig. 2b; Breckenridge et al., 2004; Fisher and Whitman, 1999; Mothersill, 1985), indicating the western and eastern parts of the Lake Superior basin were hydrologically linked. Red varves have not been clearly or consistently reported for areas of the northern Lake Superior basin. Varves are ubiquitous in the northern Lake Superior basin, however, but are gray in color, if any color is reported at all, and are usually associated with ice retreat from the lake basin altogether (Fig. 2b; Breckenridge, 2007; Breckenridge et al., 2004; Colman et al., 2020; Dell, 1973, 1976; Farrand, 1969; Halfman and Johnson, 1984; Hyodo and Longstaffe, 2011; Johnson, 1980; Johnson and Fields, 1984; Kemp et al., 1978; Landmesser et al., 1982; Maher, 1977; Mothersill, 1979, 1985, 1988; Mothersill and Fung, 1972; O'Beirne, 2013; Raymond et al., 1975; Teller and Mahnic, 1988; Thomas and Dell, 1978; Yu et

al., 2010). Where red varves are absent, gray varves directly overly pre-Marquette Readvance till or outwash, including at a
125   shallow rise just northeast of Isle Royale (gray square in Fig. 2b; Mothershill and Fung, 1982).

The landscape of Isle Royale is characterized by glacial sediments that blanket the ~1.1 Ga Portage Lake Volcanics and
Copper Harbor Conglomerate on the southwest third of the island (Fig. 3a; Davis et al., 2022; Elling et al., 2022; Huber,
1973). Glacial striae are oriented parallel to ridges and indicate northeast-to-southwest Laurentide Ice flow where bedrock is
130   exposed, but striae and craig-and-tail structures (mapped as drumlins) indicate east-to-west ice flow where bedrock is
covered by glacial drift. Striae and craig-and-tail structures point to and terminate at arcuate ice marginal deposits that mark
recessional positions of Laurentide Ice following the Marquette Readvance (Fig. 3; Huber, 1973). Strandlines of early
proglacial lakes that occupied the western Lake Superior basin (e.g. Highbridge to Shelter Bay; Figs. 3b, 4) are present at
high elevations on the island, but only on northwest-facing slopes of the island's ridges, whereas strandlines of younger
135   proglacial lakes (e.g. Huron Mtn. and younger; Figs. 3b, 4) are found on northwest- and southeast-facing slopes at lower
elevations (Breckenridge, 2013; Farrand, 1969). All striae, craig-and-tail structures, and ice-marginal landforms are found at
elevations above the younger strandlines and were thus formed by ice that covered southeast-facing slopes late into the
drawdown history of proglacial lakes (Huber, 1973). The sharp topographical expression of ice-marginal landforms is an
indication they are recessional moraines that were formed subaerially and not reworked by wave processes (Huber, 1973);
140   these moraines have never been dated.

Carbon-14 ages of organic sediments extracted from the bottoms of cores at Lily Lake and Lake Ojibway on Isle Royale's
southwest and northeast ends provide broad constraints on deglaciation of Isle Royale before ~10.7 cal ka (median age; 2σ
age range of 11.1–10.5 cal ka) and ~9.8 cal ka (median age; 2σ age range of 10.1–9.7 cal ka), respectively (Fig. 3A; Flakne,
145   2003). Paleomagnetic reconstructions and varve counting for a sediment core southwest of Isle Royale (LS00-3P; Fig. 2b),
indicate this site was ice-free by at least ~10.7 ka (Fig. 2; Breckenridge, 2007). Dated strandlines that were correlated across
the western Lake Superior basin, including Isle Royale, constrain the drawdown of Glacial Lake Duluth to post-Minong
levels to a two-century period between ~10.8–10.6 cal ka, draining first to the Lake Michigan basin via the Au Train-
Whitefish outlets and ultimately to the St. Mary's River (Figs. 2, 3b; median ages as presented in Breckenridge, 2013). Two
150   prominent subaqueous moraines (IR1 and IR2) span the western Lake Superior basin from Isle Royale to Michigan's
Keweenaw Peninsula but have never been associated with any land-based moraines nor have they been dated directly (Figs.
2, 3; Breckenridge, 2013; Colman et al., 2020; Landmesser et al., 1982). Formation of the IR2 moraine is estimated at
~10.5–10.2 ka (Colman et al., 2020), based on the presence of red varves found only on the down-ice side of IR2, the
transition from red to gray varves at the LS00-3P core (Fig. 2; Breckenridge, 2007), and correlations to the dated red-to-gray
155   varve transition in cores from the eastern Lake Superior basin (Breckenridge et al., 2004; Hyodo and Longstaffe, 2011).
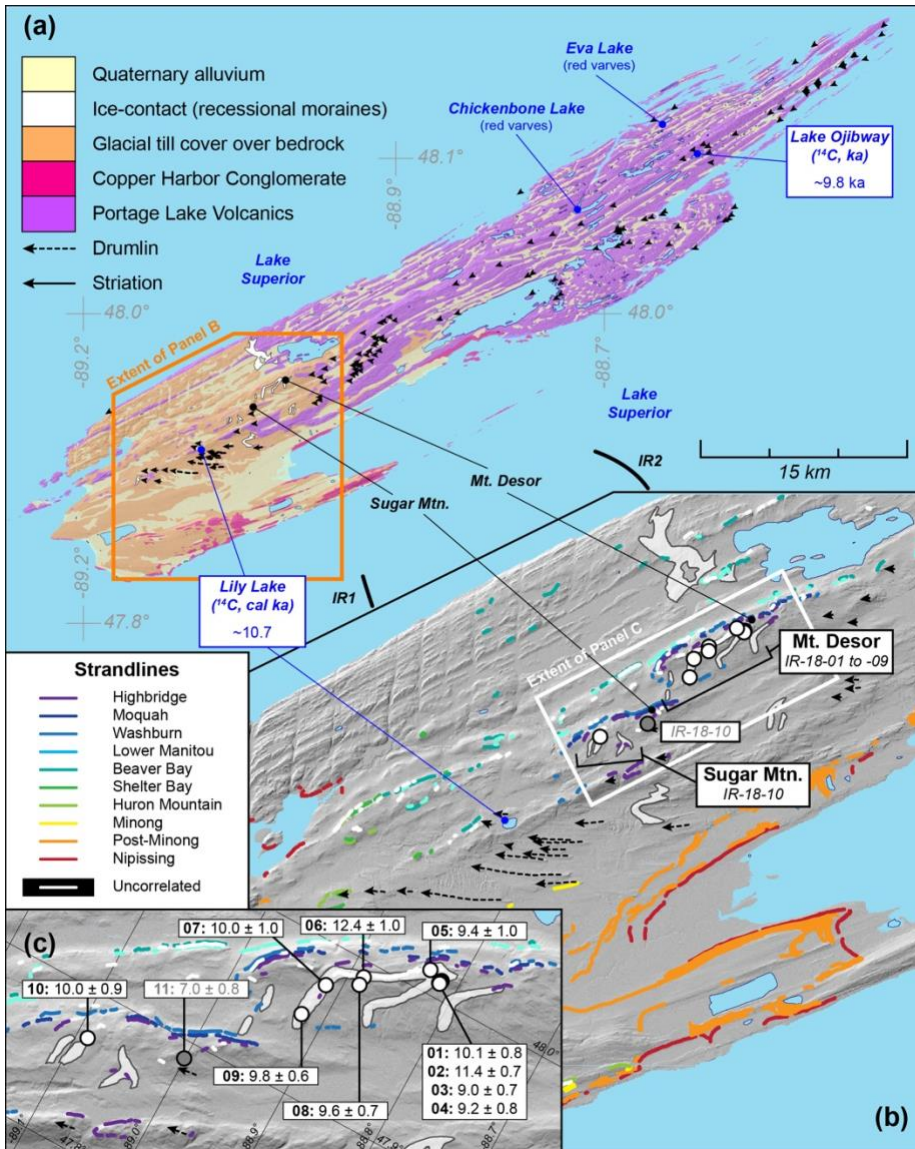
Figure 3. A. Bedrock and surficial geological map of Isle Royale (NPS, 2008), locations of subaqueous moraines IR1 and IR2 (Colman et al., 2020) and inland lakes (Flakne, 2003; Raymond et al., 1975). ^{14}C ages are median ages of the 2σ calibrated age range. B. Isle Royale's recessional moraines (Huber, 1973) and named strandlines (Breckenridge, 2013). Locations of samples from this study are shown by circles; IR-18-11 is shaded gray because it is anomalously younger than other samples and not included in the mean age of deglaciation we present for Isle Royale. C. Locations of samples relative to positions of Isle Royale's highest moraines and strandlines (see Figure 4). Bold numbers are sample IDs following the format IR-18-XX.

160

3 Methods

165 We collected samples in 2018 from the tops of quartz-bearing glacial erratics situated on the highest-elevation recessional moraines on Isle Royale (Fig. 3; Table 1; Appendix A). Nine samples were collected from moraines at Mt. Desor (IR-18-01 through IR-18-09), one sample was positioned on a small moraine near Sugar Mountain (IR-18-10), and another (IR-18-11) was positioned on an upland drift plain between the Sugar Mtn. and Mt. Desor moraines. Targeting the highest-elevation relatively high-relief moraines on Isle Royale minimizes the potential of prolonged subaqueous erratic emplacement under

170 lowering proglacial lake levels (Breckenridge, 2013). To this end, all samples collected are higher in elevation than Lily Lake, which was isolated from proglacial lakes in the Lake Superior basin by ~10.7 cal ka (median age; Flakne, 2003) while lake levels dropped from Glacial Lake Duluth to post-Minong levels ~10.8–10.6 cal ka (Figs. 3, 4; median ages presented in Breckenridge, 2013). If any of the samples were initially exposed from beneath retreating ice while underwater, they experienced less than ~100 yrs of subaqueous exposure, which is not long enough to significantly affect ^{10}Be production and

175 thus exposure ages. The tops of all erratics were >25 cm above the forest floor and eight of the eleven were >40 cm above the forest floor (Table 1).

Table 1. Sample Locations and Characteristics

Sample ID	Latitude (°N)	Longitude (°W)	Elevation[a] (m)	Shielding	Thickness (cm)	Rock type	Dimensions L x W x H (cm)
IR-18-01	47.95536	89.01206	421	0.999997	2.0	Granite	80 x 80 x 35
IR-18-02	47.98524	89.01217	421	0.999998	3.0	Granite	90 x 70 x 25
IR-18-03	47.95000	89.01228	421	0.999996	3.3	Granite	135 x 110 x 30
IR-18-04	47.95499	89.01215	421	1.000000	1.5	Granite	130 x 110 x 40
IR-18-05	47.95890	89.01457	419	0.999771	4.3	Granite	130 x 80 x 50
IR-18-06	47.95174	89.02392	412	0.999998	2.0	Granite	240 x 150 x 40
IR-18-07	47.94902	89.02894	393	0.999872	2.5	Granite	270 x 190 x 75
IR-18-08	47.95077	89.02398	401	0.999805	1.5	Granite	265 x 240 x 65
IR-18-09	47.94488	89.03035	373	0.999781	3.0	Gneiss	150 x 120 x 65
IR-18-10	47.91520	89.06030	402	0.999999	2.8	Granite	145 x 150 x 60
IR-18-11	47.93444	89.04440	387	0.997475[b]	3.8	Granite	250 x 200 x 75

[a] Elevations are present-day, meters above sea level, and are not corrected for glacial isostatic adjustment
[b] IR-18-11 was collected along the sloped top side of the erratic, which was adjacent to an even-larger mafic erratic. In addition to topographic shielding, shielding for IR-18-11 accounts for self-shielding of the erratic's sloped surface (strike 308°, dip 12°) and local horizon shielding from the adjacent erratic ([170°, 0.64], [180°, 0.86], [205°, 0.64]) using Balco et al.'s (2008) shielding calculator (wrapper 2.0, skyline 2.0).

180 Quartz was isolated from samples using froth-flotation and acid etching at the Purdue Rare Isotope Measurement (PRIME) Laboratory. Be was isolated and purified from quartz at the National Science Foundation / University of Vermont Community Cosmogenic Facility following established procedures (Corbett et al., 2016). We dissolved between 6.1 and 21.5 g of quartz and isotopically diluted each sample with ~250 μg ^{9}Be using an in-house carrier, termed UVM-SPEX, created from dilution of SPEX 10,000 ppm Be standard, with a resulting concentration of 304 ug mL^{-1} (Table 2). The eleven samples

185 were processed alongside one process blank. ^{10}Be/^{9}Be ratios were measured at PRIME in March 2022 and normalized to primary standard 07KNSTD3110, with an assumed ratio of 2.850 x 10^{-12} (Nishiizumi et al., 2007). We corrected the

measured ^{10}Be/^{9}Be ratios with the ratio and uncertainty of the one process blank and propagated uncertainties in quadrature (Table 2).

190 Exposure ages of erratics were determined in February 2023 using Balco et al.'s (2008) exposure-age calculator (version 3, default production rate) based on present-day elevations, and Lifton et al.'s (2014) LSDn ^{10}Be production rate scaling scheme. Topographic shielding for each sample was calculated in ArcGIS Pro using Li's (2018) point-based shielding tool and LiDAR imagery (pers. comm. Seth DePasqual, 2018); the sloped surface of IR-18-11 required self-shielding calculations (see footnote in Table 1). Ages assume no post-glacial erosion or burial. The effects of glacial isostatic adjustment, snow

195 cover, the use of other ^{10}Be production rates, or the use of other scaling schemes were considered through multiple sensitivity analyses and would represent differences of no more than 0.4–6.7% (see Appendix B); these small adjustments would not change our interpretation of the data.
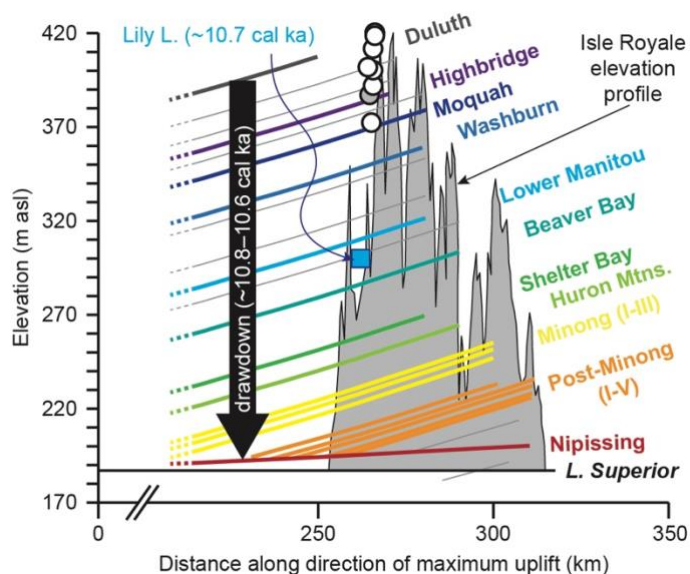
200 **Figure 4.** Average elevation profile and traces of major strandlines identified on Isle Royale (adapted from Breckenridge, 2013). Drawdown of Glacial Lake Duluth to Post-Minong stages, isolation of Lily Lake from proglacial lakes (blue square; median age; Flakne, 2003), and exposure of erratics used in this study (circles; gray circle is IR-18-11, which is not included in the mean age of deglaciation presented in this study) occurred within the ~200-year period from ~10.8–10.6 cal ka (median ages as presented in Breckenridge, 2013).

205

210

Table 2. ^{10}Be Isotopic Data and Exposure Ages

Sample Name	Quartz Mass (g)	Mass of ^{9}Be Added (µg)[a]	AMS Cathode Number	Measured ^{10}Be/^{9}Be Ratio (x10^{-14})[b]	± 1σ (x10^{-15})	Background-Corrected ^{10}Be/^{9}Be Ratio (x10^{-14})[c]	± 1σ (x10^{-15})	[^{10}Be] (at g^{-1}, X10^4)	± 1σ (x10^3)	Exposure Age (ka)[d]	± 1σ (int/ex)
IR-18-01	8.5081	250.1	162868	3.583	2.310	3.110	2.446	6.109	4.804	10.1	0.8/1.0
IR-18-02	12.5027	251.2	162869	5.575	3.224	5.102	3.322	6.849	4.460	11.4	0.7/1.0
IR-18-03	10.0280	250.3	162870	3.689	2.550	3.217	2.673	5.365	4.458	9.0	0.7/0.9
IR-18-04	7.9948	251.2	162871	3.130	2.245	2.657	2.384	5.579	5.006	9.2	0.8/1.0
IR-18-05	6.1327	250.7	162872	2.501	1.999	2.028	2.154	5.541	5.886	9.4	1.0/1.1
IR-18-06	7.1561	250.2	162874	3.617	2.468	3.145	2.596	7.348	6.065	12.4	1.0/1.3
IR-18-07	6.7303	250.7	162875	2.815	2.186	2.342	2.329	5.831	5.799	10	1.0/1.2
IR-18-08	10.0566	249.7	162876	3.923	2.286	3.450	2.423	5.723	4.020	9.6	0.7/0.9
IR-18-09	21.4996	250.4	162877	7.699	4.045	7.226	4.124	5.623	3.209	9.8	0.6/0.8
IR-18-10	8.3331	250.9	162878	3.385	2.409	2.912	2.540	5.858	5.109	10.0	0.9/1.1
IR-18-11	8.2871	249.2	162879	2.453	2.241	1.980	2.381	3.979	4.784	7.0	0.8/0.9

[a] ^{9}Be was added using an in-house carrier, termed UVM-SPEX, created from dilution of SPEX 10,000 ppm Be standard, with a resulting concentration of 304 ug mL^{-1}.

[b] Isotopic analysis was conducted at PRIME Laboratory on 8 March 2022; ratios were normalized against standard 07KNSTD3110 with an assumed ratio of 2.850 x 10^{-12} (Nishiizumi et al., 2007).

[c] Background corrections were made using one measurement blank sample. UVM Batch Number: 692; AMS Cathode Number: 162873; AMS ^{10}Be/^{9}Be blank sample ratio: 4.728E-15; ^{10}Be/^{9}Be blank sample ratio uncertainty: 8.030E-16.

[d] Exposure ages calculated using in Balco et al.'s (2008) exposure age calculator (v. 3, default production rate), Lifton et al.'s (2014) scaling scheme (LSDn), a rock density of 2.7 g cm^{-3}, present-day elevations, topographic shielding (Li, 2018), and self-shielding for one sample (IR-18-11, Table 1). Other production rate calibrations, calculators, production rate scaling schemes, snow shielding, and glacial isostatic adjustment corrections were considered but ultimately not incorporated into the ages presented here (see Supplementary Material).

4 Results

Measured concentrations of ^{10}Be from the eleven erratics range from (3.98 to 7.35) x 10^4 atoms g^{-1} (Table 2), which correspond to exposure ages of 7.0 ± 0.8 ka to 12.4 ± 1.0 ka (1σ internal uncertainties; Table 2). Samples from the Mt. Desor moraine (n = 9; IR-18-01 through IR-18-09) yield exposure ages ranging from 9.0 ± 0.7 ka to 12.4 ± 1.0 ka (1σ, internal). Sample IR-18-11, collected between the Mt. Desor and Sugar Mountain moraines, yields the youngest age of the sample set (7.0 ± 0.8 ka; 1σ, internal), and it was identified by Balco et al.'s (2008) exposure-age calculator as being an outlier from the remainder of the dataset. We did not observe any evidence of IR-18-11 having been rolled or tipped in the past, nor were there topographical indications it was exhumed. However, the young age of IR-18-11 places it out of chronological and geographic sequence between the otherwise similar exposure ages of erratics on the Mt. Desor and Sugar Mtn. moraines; therefore, we do not include IR-18-11 in our interpretations of Isle Royale deglaciation timing. After omitting the age of IR-18-11, the mean of ten samples from the Mt. Desor and Sugar Mtn. moraines is 10.1 ± 1.1 ka (1 standard deviation (SD); Fig. 5).

We present the mean age with one standard deviation uncertainties (~11% SD) because it is a conservative estimate of deglaciation timing that reflects geological uncertainty. The standard deviation of the mean age of our dataset is larger than the average shift in exposure ages that results from using any of the following: (i) a different exposure-age calculator (i.e. the

Ice-TEA exposure age calculator; 6.7% shift; Jones et al., 2019), (ii) the Northeast North America [10]Be production rate calibration (0.5% shift; Balco et al., 2009), (iii) a [10]Be production rate scaling scheme other than LSDn (0.4% to 2.2% shift), (iv) snow shielding corrections (2.9% shift), or (v) glacial isostatic adjustments (Jones et al., 2019; 3.8% shift). See Appendix B for details on age comparisons.

235 **5 Discussion**

The consistency of new [10]Be ages of erratics from the Mt. Desor and Sugar Mountain Moraines indicates they share a similar history of exposure at 10.1 ± 1.1 ka (mean, 1 SD). Ice retreat at this time implies moraine exposure later than previously proposed (i.e. Glacial Lake Beaver Bay) because it may postdate the drawdown of Glacial Lake Duluth to post-Minong stages (~10.8–10.6 cal ka, median ages; Breckenridge, 2013), which is consistent with the presumption that Isle Royale's

240 recessional moraines were deposited subaerially (Huber, 1973). This interpretation is further supported by the fact that the ages of the five lowest-elevation samples, which would have been deposited subaqueously if ice retreated prior to proglacial lake level drawdown (IR-18-06 through IR-18-10; 10.4 ± 1.1 ka, SD) are indistinguishable from the five samples that would have been exposed subaerially (IR-18-01 through IR-18-05; 9.8 ± 1.0 ka, SD), even if glacial Lake Duluth had extended this far into the western Lake Superior basin (Fig. 4).

245

The timing we infer for ice retreat from the Mt. Desor and Sugar Mtn. moraines is chronologically and geographically consistent with the timeline of presently known deglaciation events in the western Lake Superior basin. The LIS on Isle Royale's northwest side and the Thunder Bay region of Ontario retreated to Lake Nipigon by ~10.6 ka (Leydet et al., 2018; Lowell et al., 2021). Southwest of Isle Royale in Lake Superior, the LS00-3P core site records ice-free conditions by ~10.7

250 ka (Breckenridge, 2007), which is coeval with the timing of Lily Lake's isolation from proglacial lakes at ~10.7 cal ka (minimum-limiting median age; 11.1–10.5 cal ka, 2σ age range; Fig. 5; Flakne, 2003). Ages from the LS00-3P core and minimum-limiting ^{14}C ages from Lily Lake may predate ice retreat from the Mt. Desor and Sugar Mtn. moraines (~10.1 ± 1.1 ka based on the new ages we present here) and ice retreat from the subaqueous IR2 moraine south of Isle Royale (~10.5–10.2 ka; Colman et al., 2020). The timing of ice retreat from IR2 is largely consistent with the timing of ice retreat from the

255 Mt. Desor and Sugar Mtn. moraines, and we therefore suggest contemporaneous early Holocene Laurentide Ice retreat from Isle Royale and IR2.

To explain the possibility of retreat of the LIS from southern side of Isle Royale at ~10.1 ± 1.1 ka (1 SD), relatively later than ice retreat to the north, we invoke a previously proposed hypothesis that the subaqueous IR1 and IR2 moraines were

260 formed because Isle Royale and the Keweenaw Peninsula provided lateral stability to the retreating ice margin (Colman et al., 2020). Ice bracing in this location may account for the east-to-west orientation of striations and craig-and-tail structures mapped on Isle Royale (Fig. 3; Huber, 1973), and delayed ice retreat from IR1 and IR2 may explain the longer-lasting

presence of ice on Isle Royale's southeastern side compared to its northwestern side. In turn, this longer-lasting presence of
ice on Isle Royale's southeast side accounts for the lack of strandlines older than post-Minong stages on the island's
265 southeast-facing slopes (Fig. 3). Strandlines older than post-Minong stages are similarly absent from northwest-facing slopes
on the Keweenaw Peninsula across from Isle Royale (Breckenridge, 2013), though they do exist down-ice of the IR1
moraine (Hughes, 1963). The present apparent absence of strandlines older than post-Minong along the entire Keweenaw
Peninsula supports the notion of long-lasting ice cover between the two landforms until ice retreat at ~10.1 ± 1.1 ka (1 SD).
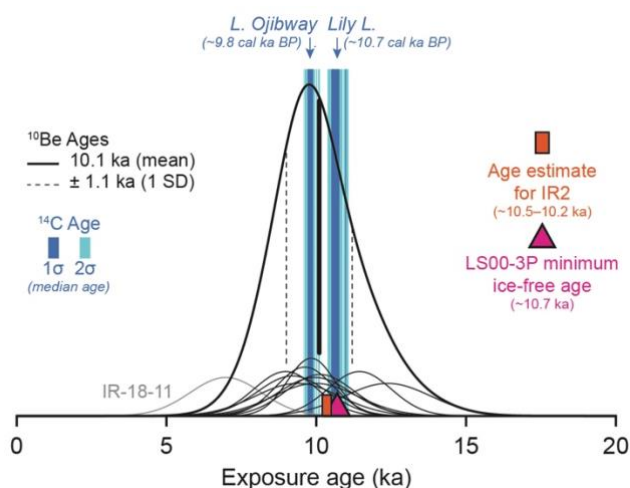
270

Figure 5. Distribution of [10]Be exposure ages from this study (exclusive of IR-18-11; see Results). Ice-free conditions at Lily
Lake and Lake Ojibway (Flakne, 2003) are shown by median ^{14}C ages and their 1σ and 2σ distributions (dark and light blue,
respectively; ^{14}C age 2σ ranges were recalibrated using CALIB rev. 8; Stuiver et al., 1993; median ages are unchanged from
original publication). Minimum ice-free conditions southwest of Isle Royale at the LS00-3P core site (pink triangle) and the
275 age estimates for the subaqueous IR2 moraine (orange rectangle) south of Isle Royale are also shown (Breckenridge, 2007;
Colman et al., 2020).

The emerging chronology of ice retreat between Isle Royale south to the Keweenaw Peninsula contrasts with the existing ice
retreat history of Lake Superior's North Shore, and we hypothesize that the margin of Laurentide Ice Sheet split along the
280 northeast-southwest axis of Isle Royale's ridges and retreated as separate ice fronts. North of Isle Royale, nearly-constant
modelled ice retreat rates of ~40–60 m yr^{-1} and retreat to the Nipigon Moraine by ~10.6 ka have been documented (Fig. 2A;
Leydet et al., 2018; Lowell et al., 2021). In contrast, ice retreat south of Isle Royale from the LS00-3P core site (~10.7 ka;
Fig. 2; Breckenridge, 2007) to the Mt. Desor and IR2 moraines (~10.1 ka; Colman et al., 2020; this study), a distance of ~60
km, indicates an ice retreat rate of ~100 m yr^{-1} that appears to outpace the mainland retreat chronology. However, ice retreat
285 south of Isle Royale paused long enough to build the ~60–100 m high IR1 and IR2 moraines during a time when proglacial
lake levels were similar to those of Glacial Lake Duluth (Colman et al., 2020), so the ~100 m yr^{-1} retreat rate we present here
is a maximum rate that does not include periods of standstill.

Continued ice retreat from Isle Royale and the IR2 moraine was rapid, exposing the inland Lake Ojibway at ~9.8 cal ka

290 (median age; Flakne, 2003), ~30 km northeast of Mt. Desor – a time that is indistinguishable from the 10.1 ± 1.1 ka (1 SD) retreat age we infer from the Sugar Mtn. and Mt. Desor moraines (Figs. 3, 5). This rapid retreat accounts for the lack of glacial depositional features on the northeastern-most two thirds of Isle Royale (Fig. 3; Huber, 1973). Regional ice retreat to the Nakina Moraine was completed by ~9 ka, exposing the entirety of the northern Lake Superior basin in less than 1 ky (Breckenridge 2007, 2013; Breckenridge et al., 2004; Colman et al., 2020; Hyodo and Longstaffe, 2011; Kelly et al., 2016;

295 Lowell et al., 2021; Teller and Mahnic, 1988) and sites between Lake Superior's North Shore and the Nakina Moraine (Fig. 6d; Bajc et al., 1997; Saarnisto, 1974). This inferred retreat timing, extrapolated over the >300 km distance from Isle Royale and the IR2 moraine to the Nakina moraine, means ice retreat rates south of Isle Royale nearly tripled to ~270 m yr^{-1} as the ice margin retreated across deep waters of northern Lake Superior.

300 Division of the retreating LIS margin into two separate retreating fronts, northwest and southeast of Isle Royale in the early Holocene has implications for meltwater routing and the Lake Superior lake-bottom stratigraphy. Red varves associated with influx of meltwater from Glacial Lake Agassiz were identified down-ice of the subaqueous IR2 moraine south of Isle Royale, but not up-ice (Fig. 2B). Colman et al. (2020) interpreted this to mean gray varve deposition across Lake Superior was associated specifically with ice retreat from the IR2 moraine, not from the Lake Superior basin itself (Farrand, 1969).

305 Following Colman et al.'s (2020) interpretation, the similar ages of Isle Royale's recessional moraines and IR2 implies that the presence of red varves across the Lake Superior basin delineates a regional ice margin when ice was last present on Isle Royale. Previously drawn retreat positions place the LIS margin across the northern Lake Superior basin by ~10.5 ka (Fig. 2; Breckenridge, 2013), but red varves do not seem to be present in Nipigon Bay nor the northern Lake Superior basin (Fig. 2), and gray varves are identified directly overlying till (i.e. no red varves) at a shallow rise immediately northeast of Isle Royale

310 (Fig. 2b; Mothersill and Fung, 1972). We suggest that water in the western Lake Superior basin was blocked from draining north around both Isle Royale and the Keweenaw Peninsula by the longer-lasting ice on Isle Royale and the IR2 moraine (Fig. 6). In this case, meltwater from glacial Lake Agassiz would have drained into the western Lake Superior basin at Black Bay and then drained across the Keweenaw Peninsula to the eastern Lake Superior basin via the Portage and Allouez outlets, where are known to have previously carried water, but have not been dated (Hughes, 1963). We propose that the drawdown

315 of Glacial Lake Duluth to post-Minong stages was through the Portage and Allouez outlets, which were subsequently abandoned following the rapid ice retreat from Isle Royale and IR2 that exposed the rest of the present Lake Superior basin (Fig. 6).

Based on the sum of new and existing chronological data and the existing regional stratigraphy, we suggest that prior to

320 rapid ice retreat from Isle Royale, the LIS margin extended from the Nipigon Moraine to the north end of Isle Royale, followed the island's ridges to recessional moraines dated in this study, then traversed the Lake Superior basin along the IR2 moraine (Colman et al., 2020), linking Isle Royale and the Keweenaw Peninsula until ice retreat at 10.1 ± 1.1 ka (n = 10,

average, 1 SD; Fig. 6). This interpretation places the southwest margins of Laurentide Ice Sheet in contact with the southern shores of Lake Superior until ice retreat at ~10.1 ± 1.1 kaAt the same time, the Laurentide Ice margin on the east side of

325   Lake Superior had retreated north of Alfies Lake (median age ~10.2 cal ka; Saarnisto, 1974), so the ice margin likely arced from the Keweenaw Peninsula to the vicinity of the Chapleau Moraine (Fig. 6).
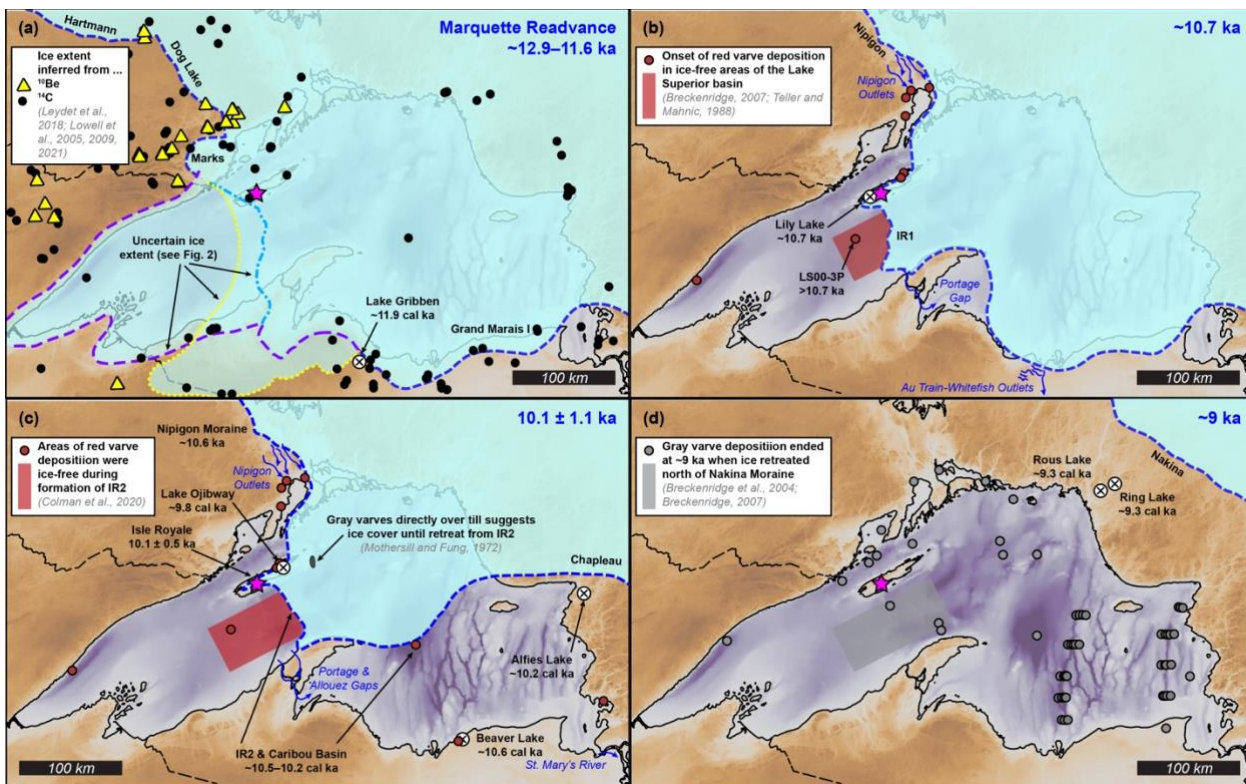
Figure 6. Laurentide Ice Sheet margins during selected time-slices following the Marquette Readvance. A. Ice margins

330   confidently associated with the Marquette Readvance are placed along the Grand Marais I, Marks, Dog Lake, and Hartmann moraines based on regional [10]Be and ^{14}C ages (yellow triangles and black dots, respectively; Dalton et al., 2020; Leydet et al., 2018; Lowell et al., 1999, 2005, 2009, 2021). There is currently less certainty for the placement of ice margins around the western Lake Superior basin (yellow, blue, and purple dashed lines; Clayton and Moran, 1982; Colman et al., 2020; Drexler et al., 1983; Hughes and Merry, 1978; Peterson, 1985). B. First red varve deposition observed for western Lake

335   Superior Basin before ~10.7 ka (Breckenridge, 2007; Colman et al., 2020; Flakne, 2003; Maher, 1977; Teller and Mahnic, 1988). C. Final red varve deposition, prior to transition to gray varve deposition and ice margins within the uncertainty of [10]Be exposure ages presented in this study (Breckenridge, 2007; Colman et al., 2020; Fisher et al., 1999; Flakne, 2003; Mothersill et al., 1985; Saarnisto, 1974). D. Lake cores preserving gray varve deposition across Lake Superior following ice retreat from Isle Royale and IR2 (Dell, 1976; Breckenridge 2007; Breckenridge et al., 2004; Colman et al., 2020; Fisher and

340   Whitman, 1999; Halfman and Johnson, 1984; Hyodo and Longstaffe, 2011; Johnson and Fields, 1984; Maher, 1977; O'Beirne, 2013; Raymond et al., 1975; Teller and Mahnic, 1988; Yu et al., 2010). Most gray varve sections across end with a correlative sequence of 36 anomalously thick varves at ~9 ka; these thick varves are associated with the final pulses of meltwater from the LIS before it retreated from the Nakina moraine (Breckenridge et al., 2004). Minimum-limiting ages (cal ka) of Rous Lake and Ring Lake are median ages of organic sediment (Bajc et al., 1997; Saarnisto, 1974).

345 6 Implications

New [10]Be exposure ages from recessional moraines on Isle Royale in Lake Superior expand the geographical coverage of quantitative age constraints on the timing of LIS retreat from the Great Lakes (Fig. 6). The new model we propose for the position of Laurentide Ice in the early Holocene unifies ice retreat chronologies along Lake Superior's North Shore with undated subaqueous landforms and the Lake Superior south shore along the Keweenaw Peninsula. By inferring that

350 Laurentide Ice remained in contact with the Keweenaw Peninsula into the early Holocene, we further clarify the relationship between the position of the ice margin, meltwater drainage pathways, and spatial patterns in lake-bottom stratigraphy. Interpretations drawn from the dataset presented here demonstrate that dating glacial features on islands in large lake can be integral to reconstructing regional patterns of deglaciation across bodies of water and bridging relationships between subaerial and subaqueous glacial landforms.

355 Appendix A: Photographs of sample sites

Glacial erratics are common across Isle Royale. Those suitable for [10]Be exposure age dating are easily identifiable because they are often granite or metamorphic rocks from the Canadian Shield, which stand in stark contrast to the mafic igneous and volcaniclastic rocks comprising the bedrock of Isle Royale. Most erratics are smaller than those typically found in Alpine environments because of the long transport distances from their sources. During the three days of fieldwork on Isle Royale,

360 many erratics were identified but only those most suitable for dating were sampled. Sampled erratics were those positioned on moraine crests or broad uplands with minimal topographic shielding and least likely to have rolled down hills or have complex exposure and/or burial histories (Fig. A1).

365 **Figure A1.** Photographs of the eleven samples used in this study. Rock hammers, plastic zip bags, GPS units, and people are present for scale.

Appendix B: Sensitivity analyses of exposure-age calculation decisions

In this study, we present exposure ages that were calculated using the online exposure-age calculator presented by Balco et al. (2008; vers. 3) using the default [10]Be production rate calibration and the LSDn [10]Be production rate scaling scheme

370 (Lifton et al., 2014). Standard [10]Be production shielding corrections were made (Table 1), but we do not incorporate any other production rate scaling options nor use a regional [10]Be calibration dataset. In each section of Appendix B, we explore how [10]Be exposure ages from Isle Royale would have shifted had we made different decisions. Importantly, calculating ages with any of these adjustments only results in minor changes in exposure ages and would not alter the results of this study.

375 **B.1 Choice of exposure-age calculator**

We considered the use of two online calculators, the first presented by Balco et al. (2008), which is regularly updated, and the newer Ice-TEA calculator (Jones et al., 2019). Both calculators follow the guiding principles of cosmogenic nuclide production (Gosse and Phillips, 2001), but with recognized differences, including how atmospheric pressure is incorporated into age calculations or how easily users can choose regional production rate calibration datasets. Differences in calibration

380 datasets have led to differences in exposure ages from the same input data for at least one previous study in the Great Lakes

region (e.g. Lowell et al., 2021). In this study, exposure ages calculated with the Ice-TEA calculator are, on average, 6.7%

older (range: 5.8% to 7.0%) than ages calculated using Balco et al.'s calculator (Table B1). We chose to present ages from

Balco et al. (2008)'s calculator, primarily because of its longevity and because it is used by other [10]Be exposure-age studies

in the Great Lakes region.

385

| Table B1. Exposure ages calculated using Balco et al. (2008) versus Ice-TEA | | | | | | |
| Sample ID | Balco et al. (2008) | | | Ice-TEA (Jones et al., 2019) | | |
	Age (ka)	± 1σ (int.)	± 1σ (ext.)	Age (ka)	± 1σ (int.)	± 1σ (ext.)	% diff.
IR-18-01	10126	798	998	10820	940	1260	6.9%
IR-18-02	11446	747	1009	12250	790	1250	7.0%
IR-18-03	8979	748	917	9580	830	1110	6.7%
IR-18-04	9207	828	991	9820	910	1220	6.7%
IR-18-05	9374	998	1142	10020	1080	1350	6.9%
IR-18-06	12385	1025	1260	13140	1100	1470	6.1%
IR-18-07	9973	994	1156	10660	1080	1370	6.9%
IR-18-08	9619	677	884	10280	760	1090	6.9%
IR-18-09	9831	562	809	10510	590	1010	6.9%
IR-18-10	9954	870	1051	10630	970	1290	6.8%
IR-18-11	6982	841	937	7390	860	1030	5.8%

B.2 Choice of [10]Be production rate calibration

Previous [10]Be exposure-age studies in the Great Lakes region (e.g. Leydet et al., 2018; Lowell et al., 2021) used the

Northeast North America (NENA) calibration for [10]Be production rates (Balco et al., 2009), which results in exposure ages

390 that are each 0.5% younger than those we use in determining the mean exposure age of deglaciation from Isle Royale (Table

B2). Although the samples we collected from Isle Royale are ice-marginal landforms found at relative high latitudes (~48°N)

and at elevations <1,000 m asl, we use the default [10]Be calibration production rate in our age calculations using Balco et al.'s

(2008) calculator, primarily because of our distance from NENA calibration sites.

| Table B2. Exposure ages calculated in Balco et al. (2008) using the default versus Northeast North America calibration datasets | | | | | | |
| Sample ID | Default production rate calibration | | | Northeast North America calibration | | |
	Age (ka)	± 1σ (int.)	± 1σ (ext.)	Age (ka)	± 1σ (int.)	± 1σ (ext.)	% diff.
IR-18-01	10126	798	998	10079	795	1157	0.5%
IR-18-02	11446	747	1009	11389	744	1207	0.5%
IR-18-03	8979	748	917	8936	744	1053	0.5%
IR-18-04	9207	828	991	9164	824	1124	0.5%
IR-18-05	9374	998	1142	9330	993	1262	0.5%
IR-18-06	12385	1025	1260	12318	1020	1448	0.5%
IR-18-07	9973	994	1156	9925	989	1290	0.5%
IR-18-08	9619	677	884	9572	674	1045	0.5%
IR-18-09	9831	562	809	9783	560	990	0.5%
IR-18-10	9954	870	1051	9906	866	1197	0.5%
IR-18-11	6982	841	937	6950	837	1018	0.5%

395

B.3 Choice of [10]Be production rate scaling scheme

Previous studies present exposure ages using different production rate scaling schemes including non-time-dependent scaling based on atmospheric measurements (St; Lal, 1991; Stone, 2000) and time-dependent scaling based on atmospheric

400 measurements and paleomagnetic reconstructions (Lm; Lal, 1991; Nishiizumi et al., 1989; Stone, 2000). Our preference of [10]Be production rate scaling is to use Lifton et al.'s (2014) LSDn scaling scheme because it accounts for changes in the strength of Earth's magnetosphere, changes in solar cosmic ray output, and numerous cosmogenic isotope production pathways (LSDn; Lifton et al., 2014).Exposure ages of erratics on Isle Royale based on non-time-dependent spallogenic scaling (St) are on average 0.4% older (range: 0.2% to 0.7%) and exposure ages based on time-dependent spallogenic scaling

405 (Lm) are on average 2.2% younger (range: 2.0% to 2.8%) than ages derived using Lifton et al.'s (2014) LSDn scaling scheme (Table B3).

Table B3. Exposure ages calculated in Balco et al. (2008) using difference [10]Be production rate scaling schemes

Sample ID	LSDn Age (ka)	± 1σ (int.)	± 1σ (ext.)	St Age (ka)	± 1σ (int.)	± 1σ (ext.)	% diff.	Lm Age (ka)	± 1σ (int.)	± 1σ (ext.)	% diff.
IR-18-01	10126	798	998	10156	801	1135	0.3%	9911	781	1080	2.1%
IR-18-02	11446	747	1009	11483	750	1179	0.3%	11186	730	1114	2.3%
IR-18-03	8979	748	917	9015	751	1036	0.4%	8797	733	987	2.0%
IR-18-04	9207	828	991	9238	831	1107	0.3%	9017	811	1057	2.1%
IR-18-05	9374	998	1142	9405	1001	1248	0.3%	9180	977	1196	2.1%
IR-18-06	12385	1025	1260	12328	1021	1413	0.5%	12039	997	1347	2.8%
IR-18-07	9973	994	1156	9996	996	1273	0.2%	9755	972	1218	2.2%
IR-18-08	9619	677	884	9657	680	1023	0.4%	9428	664	971	2.0%
IR-18-09	9831	562	809	9856	564	963	0.3%	9621	550	909	2.1%
IR-18-10	9954	870	1051	9978	872	1177	0.2%	9736	851	1123	2.2%
IR-18-11	6982	841	937	6936	835	1000	0.7%	6794	818	964	2.7%

410 ## B.4 Effects of snow shielding

Previous [10]Be studies in the region used sample collection strategies to minimize the potential of snow-shielding (e.g. unforested, windswept, high-elevation locations; Leydet et al., 2018; Lowell et al., 2021); this was not an option on Isle Royale. Given its position in the middle of Lake Superior, heavy lake effect snow is probable on Isle Royale, and the forest at the Mt. Desor and Sugar Mountain Moraines may prevent fallen snow from blowing away easily. We considered the

415 effects of snow-shielding at our sample sites using average monthly snow-depth totals that were measured at Isle Royale's Mott Island Station:

- Station: #205637 (National Climatic Data Center, NCDC)
- Location: 48°06' N, 88°33' W
- Elevation: 610 ft above sea level

420
- Period of record: 01 October 1940 to 29 April 2016 (41.8% of possible observations reported, Table B4)
- Data access: Western Regional Climate Center, https://wrcc.dri.edu/ (last accessed 22 February 2023)

Snow shielding calculations are based on Eq. (3.76) in Gosse and Phillips (2001):

425 $S_{snow} = \frac{1}{12} \sum_{i}^{12} e^{-(z_{snow,i}\, \rho_{snow,i}\, /\Lambda)}$,

Here, $z_{snow,i}$ is the monthly average snow thickness above the ground (cm), $\rho_{snow,i}$ is the monthly average snow density (g cm^{-3}), and Λ is attenuation of cosmic rays (160 g cm^{-2}). We use an average old-age snow density of 0.27 g cm^{-3} measured from Isle Royale (Peterson, 1977).

430

Table B4. Monthly average snow depth at Mott Island (October 1940–April 2016)

	Jan	Feb	Mar	Apr	May	Jun	Jul	Aug	Sep	Oct	Nov	Dec
Reported (inches)	13	23	25	10	0	0	0	0	0	0	2	8
For shielding calculations (cm)	33.0	58.4	63.5	25.4	0	0	0	0	0	0	5.1	20.3

Including snow shielding led to exposure ages that were, on average, 2.9% older (range: 2.6% to 3.3%) than without snow shielding (Table B5). We choose not to include these ages in our analysis because measured snowfall from 1940 to 2016 may not accurately reflect Holocene averages.

435

Table B5. Exposure ages calculated in Balco et al. (2008) without versus with snow shielding

Sample ID	Without snow shielding			With snow shielding			% diff.
	Age (ka)	± 1σ (int.)	± 1σ (ext.)	Age (ka)	± 1σ (int.)	± 1σ (ext.)	
IR-18-01	10126	798	998	10413	821	1026	2.8%
IR-18-02	11446	747	1009	11793	770	1039	3.0%
IR-18-03	8979	748	917	9238	769	944	2.9%
IR-18-04	9207	828	991	9463	851	1019	2.8%
IR-18-05	9374	998	1142	9630	1025	1173	2.7%
IR-18-06	12385	1025	1260	12791	1059	1302	3.3%
IR-18-07	9973	994	1156	10254	1022	1189	2.8%
IR-18-08	9619	677	884	9903	697	911	3.0%
IR-18-09	9831	562	809	10113	579	832	2.9%
IR-18-10	9954	870	1051	10234	895	1080	2.8%
IR-18-11	6982	841	937	7167	863	962	2.6%

B.5 Effects of glacial isostatic adjustment

Sample sites in this study are ~300 km up-ice of the Laurentide Ice Sheet's Last Glacial Maximum terminal moraines (Ullman et al., 2015) and strandlines of proglacial lakes that once occupied the western Lake Superior basin have

440 experienced considerable uplift (Breckenridge, 2013; Farrand, 1969). In considering the effects of glacial isostatic adjustment (GIA) on the exposure ages presented in this study, we compare exposure ages from all samples using only the Ice-TEA software package's "Correct for Elevation Change" tool and the ICE-6G GIA model (Jones et al., 2019; Peltier et

al., 2015). GIA-corrected ages are compared to uncorrected ages. Exposure ages with GIA-corrections were on average 3.8% older (range: 1.1% to 8.1%) than exposure ages uncorrected for GIA (Table B6). Following Lowell et al. (2021), we choose

445 to use exposure ages uncorrected for GIA to maintain regional comparability of exposure-age datasets.

Table B6. Exposure ages calculated in Ice-TEA without versus with glacial isostatic adjustment corrections

Sample ID	Without GIA adjustment		With GIA adjustment		
	Age (ka)	± 1σ (int.)	Age (ka)	± 1σ (int.)	% diff.
IR-18-01	10820	940	11240	1430	3.9%
IR-18-02	12250	790	13020	1600	6.3%
IR-18-03	9580	830	9830	1280	2.6%
IR-18-04	9820	910	10110	1300	3.0%
IR-18-05	10020	1080	10310	1470	2.9%
IR-18-06	13140	1100	14210	2060	8.1%
IR-18-07	10660	1080	11060	1560	3.8%
IR-18-08	10280	760	10610	1230	3.2%
IR-18-09	10510	590	10880	1230	3.5%
IR-18-10	10630	970	11020	1450	3.7%
IR-18-11	7390	860	7470	1020	1.1%

Data Availability

450 All data required to reproduce the results and analyses of this study are presented in data tabled herein. Topographic shielding was done using LiDAR elevation datasets provided by the US National Park Service (pers. comm. Seth DePasqual).

Sample Availability

All sample material removed from Isle Royale National Park was destroyed in sample preparation and [10]Be extraction at Purdue University's PRIME lab and the University of Vermont Community Cosmogenic Facility.

455 ## Author Contribution

EWP: Conceptualization, formal analysis, funding acquisition, investigation, project administration, visualization, writing – original draft preparation. DJU: Formal analysis, investigation, photographs, writing – original draft preparation. LBC: Data curation, formal analysis, investigation, writing – original draft preparation. PRB: Formal analysis, investigation, resources, writing – original draft preparation. MC: Data curation, funding acquisition, resources, writing – original draft preparation.

460 ## Competing Interests

The authors declare that they have no conflict of interest.

Acknowledgements

465 This study was conducted on Isle Royale, which is a Traditional Cultural Property of the Grand Portage Band of Lake Superior Chippewa, who call the island, "Minong." We thank Mark Romanski and Seth Depasqual from Isle Royale National Park for providing sample collection permit approval and LiDAR imagery, respectively. Stephen Ogden helped with sample collection. Funding for this project was through an Eastern Michigan University Faculty Research Fellowship

and a PRIME Laboratory Seed Data Grant, both awarded to EWP. Sample processing at the NSF/UVM CCF supported by
NSF EAR-1735676.

470 **References**

Bajc, A. F., Morgan, A. V., and Warner, B. G.: Age and paleoecological significance of an early postglacial fossil
assemblage near Marathon, Ontario, Canada, Can. J. Earth Sci., 34, 687–698, https://doi.org/10.1139/e17-055, 1997.

Balco, G., Briner, J., Finkel, R. C., Rayburn, J. A., Ridge, J. C., and Schaefer, J. M.: Regional beryllium-10 production rate
calibration for late-glacial northeastern North America, Quaternary Geochronology, 4, 93–107,
475 https://doi.org/10.1016/j.quageo.2008.09.001, 2009.

Balco, G., Stone, J. O., Lifton, N. A., and Dunai, T. J.: A complete and easily accessible means of calculating surface
exposure ages or erosion rates from 10Be and 26Al measurements, Quaternary Geochronology, 3, 174–195,
https://doi.org/10.1016/j.quageo.2007.12.001, 2008.

Black, R. F.: Quaternary geology of Wisconsin and contiguous Upper Michigan, in: Quaternary stratigraphy of North
480 America, edited by: Mahaney, W. C., Dowden, Hutchinson & Ross ; exclusive distributor, Halsted Press, Stroudsburg,
Pa. : [New York], 1976.

Borchers, B., Marrero, S., Balco, G., Caffee, M., Goehring, B., Lifton, N., Nishiizumi, K., Phillips, F., Schaefer, J., and
Stone, J.: Geological calibration of spallation production rates in the CRONUS-Earth project, Quaternary
Geochronology, 31, 188–198, https://doi.org/10.1016/j.quageo.2015.01.009, 2016.

485 Breckenridge, A., Lowell, T. V., Peteet, D., Wattrus, N., Moretto, M., Norris, N., and Dennison, A.: A new glacial varve
chronology along the southern Laurentide Ice Sheet that spans the Younger Dryas–Holocene boundary, Geology, 49,
283–288, https://doi.org/10.1130/G47995.1, 2021.

Breckenridge, A.: An analysis of the late glacial lake levels within the western Lake Superior basin based on digital
elevation models, Quat. res., 80, 383–395, https://doi.org/10.1016/j.yqres.2013.09.001, 2013.

490 Breckenridge, A.: The Lake Superior varve stratigraphy and implications for eastern Lake Agassiz outflow from 10,700 to
8900 cal ybp (9.5–8.0 14C ka), Palaeogeography, Palaeoclimatology, Palaeoecology, 246, 45–61,
https://doi.org/10.1016/j.palaeo.2006.10.026, 2007.

Breckenridge, A.: The timing of regional Lateglacial events and post-glacial sedimentation rates from Lake Superior,
Quaternary Science Reviews, 23, 2355–2367, https://doi.org/10.1016/j.quascirev.2004.04.007, 2004.

495 Broecker, W. S., Kennett, J. P., Flower, B. P., Teller, J. T., Trumbore, S., Bonani, G., and Wolfli, W.: Routing of meltwater
from the Laurentide Ice Sheet during the Younger Dryas cold episode, Nature, 341, 318–321,
https://doi.org/10.1038/341318a0, 1989.

Broecker, W. S.: Was the Younger Dryas Triggered by a Flood?, Science, 312, 1146–1148,
https://doi.org/10.1126/science.1123253, 2006.

500 Carlson, A. E., Clark, P. U., Haley, B. A., Klinkhammer, G. P., Simmons, K., Brook, E. J., and Meissner, K. J.: Geochemical
proxies of North American freshwater routing during the Younger Dryas cold event, Proc. Natl. Acad. Sci. U.S.A., 104,
6556–6561, https://doi.org/10.1073/pnas.0611313104, 2007.

Carlson, A. E.: What Caused the Younger Dryas Cold Event?, Geology, 38, 383–384,
https://doi.org/10.1130/focus042010.1, 2010.

505 Ceperley, E. G., Marcott, S. A., Rawling, J. E., Zoet, L. K., and Zimmerman, S. R. H.: The role of permafrost on the
morphology of an MIS 3 moraine from the southern Laurentide Ice Sheet, Geology, 47, 440–444,
https://doi.org/10.1130/G45874.1, 2019.

Clark, P. U. and Mix, A. C.: Ice sheets and sea level of the Last Glacial Maximum, Quaternary Science Reviews, 21, 1–7,
https://doi.org/10.1016/S0277-3791(01)00118-4, 2002.

510 Clark, P. U., Dyke, A. S., Shakun, J. D., Carlson, A. E., Clark, J., Wohlfarth, B., Mitrovica, J. X., Hostetler, S. W., and
McCabe, A. M.: The Last Glacial Maximum, Science, 325, 710–714, https://doi.org/10.1126/science.1172873, 2009.

Clayton, L. and Moran, S. R.: Chronology of late wisconsinan glaciation in middle North America, Quaternary Science
Reviews, 1, 55–82, https://doi.org/10.1016/0277-3791(82)90019-1, 1982.

Colgan, P. M., Bierman, P. R., Mickelson, D. M., and Caffee, M.: Variation in glacial erosion near the southern margin of
515 the Laurentide Ice Sheet, south-central Wisconsin, USA: Implications for cosmogenic dating of glacial terrains,

    Geological Society of America Bulletin, 114, 1581–1591, https://doi.org/10.1130/0016-7606(2002)114<1581:VIGENT>2.0.CO;2, 2002.

Colman, S. M., Breckenridge, A., Zoet, L. K., Wattrus, N. J., and Johnson, T. C.: Moraines and late-glacial stratigraphy in central Lake Superior, Quat. res., 98, 19–35, https://doi.org/10.1017/qua.2020.36, 2020.

520   Corbett, L. B., Bierman, P. R., and Rood, D. H.: An approach for optimizing in situ cosmogenic 10Be sample preparation, Quaternary Geochronology, 33, 24–34, https://doi.org/10.1016/j.quageo.2016.02.001, 2016.

Cutler, P. M., Mickelson, D. M., Colgan, P. M., MacAyeal, D. R., and Parizek, B. R.: Influence of the Great Lakes on the dynamics of the southern Laurentide ice sheet: Numerical experiments, Geol, 29, 1039, https://doi.org/10.1130/0091-7613(2001)029<1039:IOTGLO>2.0.CO;2, 2001.

525   Dalton, A. S., Margold, M., Stokes, C. R., Tarasov, L., Dyke, A. S., Adams, R. S., Allard, S., Arends, H. E., Atkinson, N., Attig, J. W., Barnett, P. J., Barnett, R. L., Batterson, M., Bernatchez, P., Borns, H. W., Breckenridge, A., Briner, J. P., Brouard, E., Campbell, J. E., Carlson, A. E., Clague, J. J., Curry, B. B., Daigneault, R.-A., Dubé-Loubert, H., Easterbrook, D. J., Franzi, D. A., Friedrich, H. G., Funder, S., Gauthier, M. S., Gowan, A. S., Harris, K. L., Hétu, B., Hooyer, T. S., Jennings, C. E., Johnson, M. D., Kehew, A. E., Kelley, S. E., Kerr, D., King, E. L., Kjeldsen, K. K., 530   Knaeble, A. R., Lajeunesse, P., Lakeman, T. R., Lamothe, M., Larson, P., Lavoie, M., Loope, H. M., Lowell, T. V., Lusardi, B. A., Manz, L., McMartin, I., Nixon, F. C., Occhietti, S., Parkhill, M. A., Piper, D. J. W., Pronk, A. G., Richard, P. J. H., Ridge, J. C., Ross, M., Roy, M., Seaman, A., Shaw, J., Stea, R. R., Teller, J. T., Thompson, W. B., Thorleifson, L. H., Utting, D. J., Veillette, J. J., Ward, B. C., Weddle, T. K., and Wright, H. E.: An updated radiocarbon-based ice margin chronology for the last deglaciation of the North American Ice Sheet Complex, Quaternary Science 535   Reviews, 234, 106223, https://doi.org/10.1016/j.quascirev.2020.106223, 2020.

Davis, W. R., Collins, M. A., Rooney, T. O., Brown, E. L., Stein, C. A., Stein, S., and Moucha, R.: Geochemical, petrographic, and stratigraphic analyses of the Portage Lake Volcanics of the Keweenawan CFBP: implications for the evolution of main stage volcanism in continental flood basalt provinces, SP, 518, 67–100, https://doi.org/10.1144/SP518-2020-221, 2022.

540   Dell, C. I.: A special mechanism for varve formation in a glacial lake, Journal of Sedimentary Research, 43, 838–840, 1973.

Dell, C. I.: Sediment Distribution and Bottom Topography of Southeastern Lake Superior, Journal of Great Lakes Research, 2, 164–176, https://doi.org/10.1016/S0380-1330(76)72283-4, 1976.

Drexler, C. W., Farrand, W. R., and Hughes, J. D.: Correlation of glacial lakes in the Superior basin with eastward discharge events from Lake Agassiz, in: Glacial Lake Agassiz, vol. 26, Geological Association of Canada, 309–329, 1983.

545   Drexler, C. W.: Outlet Channels for the Post-Duluth Lakes in the Upper Peninsula of Michigan, Ph.D., University of Michigan, Ann Arbor, MI, 407 pp., 1981.

Dyke, A. S.: An outline of North American deglaciation with emphasis on central and northern Canada, in: Developments in Quaternary Sciences, vol. 2, Elsevier, 373–424, https://doi.org/10.1016/S1571-0866(04)80209-4, 2004.

Ehlers, J., Gibbard, P. L., and Hughes, P. D. (Eds.): Quaternary glaciations - extent and chronology: a closer look, Elsevier, 550   Amsterdam ; Boston, 1108 pp., 2011.

Elling, R., Stein, S., Stein, C., and Gefeke, K.: Three Major Failed Rifts in Central North America: Similarities and Differences, GSAT, 32, 4–11, https://doi.org/10.1130/GSATG518A.1, 2022.

Farrand, W. R. and Drexler, C. W.: Late Wisconsinan and Holocene history of the Lake Superior basin, Quaternary Evolution of the Great Lakes, 30, 17–32, 1985.

555   Farrand, W. R.: The Quaternary history of Lake Superior, in: Proceedings of the 12th Conference of Great Lakes Research, 181–197, 1969.

Fisher, T. G. and Whitman, R. L.: Deglacial and Lake Level Fluctuation History Recorded in Cores, Beaver Lake, Upper Peninsula, Michigan, Journal of Great Lakes Research, 25, 263–274, https://doi.org/10.1016/S0380-1330(99)70735-5, 1999.

560   Fisher, T. G., Dziekan, M. R., McDonald, J., Lepper, K., Loope, H. M., McCarthy, F. M. G., and Curry, B. B.: Minimum limiting deglacial ages for the out-of-phase Saginaw Lobe of the Laurentide Ice Sheet using optically stimulated luminescence (OSL) and radiocarbon methods, Quat. res., 97, 71–87, https://doi.org/10.1017/qua.2020.12, 2020.

Fisher, T. G.: Megaflooding associated with glacial Lake Agassiz, Earth-Science Reviews, 201, 102974, https://doi.org/10.1016/j.earscirev.2019.102974, 2020.

565 Flakne, R.: The Holocene vegetation history of Isle Royale National Park, Michigan, U.S.A., Can. J. For. Res., 33, 1144–
      1166, https://doi.org/10.1139/x03-063, 2003.

Gosse, J. C. and Phillips, F. M.: Terrestrial in situ cosmogenic nuclides: theory and application, Quaternary Science
      Reviews, 20, 1475–1560, https://doi.org/10.1016/S0277-3791(00)00171-2, 2001.

Halfman, J. D. and Johnson, T. C.: Enhanced Atmospheric Circulation over North America During the Early Holocene:
570   Evidence from Lake Superior, Science, 224, 61–63, https://doi.org/10.1126/science.224.4644.61, 1984.

Hanson, B. and Hooke, R. LeB.: Glacier calving: a numerical model of forces in the calving-speed/water-depth relation, J.
      Glaciol., 46, 188–196, https://doi.org/10.3189/172756500781832792, 2000.

Hobbs, H. C. and Breckenridge, A.: Ice advances and retreats, inlets and outlets, sediments and strandlines of the western
      Lake Superior basin, in: Archean to Anthropocene: Field Guides to the Geology of the Mid-Continent of North
575   America, Geological Society of America, 299–315, https://doi.org/10.1130/2011.0024(14), 2011.

Huber, N. K.: Glacial and post glacial geological history of Isle Royale National Park, Michigan, 1973.

Hughes, J. D.: Physiography of a six quadrangle area in the Keweenaw Peninsula north of Portage Lake, Ph.D.,
      Northwestern University, Evanston, IL, 255 pp., 1963.

Hyodo, A. and Longstaffe, F. J.: The chronostratigraphy of Holocene sediments from four Lake Superior sub-basins, Can. J.
580   Earth Sci., 48, 1581–1599, https://doi.org/10.1139/e11-060, 2011.

IAGLR: Large Lakes of the World, 2012.

Johnson, T. C. and Fields, J.: Paleomagnetic dating of postglacial sediment, offshore Lake Superior, Minnesota—Wisconsin,
      U.S.A., Chemical Geology, 44, 253–265, https://doi.org/10.1016/0009-2541(84)90076-7, 1984.

Johnson, T. C.: Late-Glacial and Postglacial Sedimentation in Lake Superior Based on Seismic-Reflection Profiles, Quat.
585   res., 13, 380–391, https://doi.org/10.1016/0033-5894(80)90064-2, 1980.

Jones, R. S., Small, D., Cahill, N., Bentley, M. J., and Whitehouse, P. L.: iceTEA: Tools for plotting and analysing
      cosmogenic-nuclide surface-exposure data from former ice margins, Quaternary Geochronology, 51, 72–86,
      https://doi.org/10.1016/j.quageo.2019.01.001, 2019.

Kelly, M. A., Fisher, T. G., Lowell, T. V., Barnett, P. J., and Schwartz, R.: 10 Be ages of flood deposits west of Lake
590   Nipigon, Ontario: evidence for eastward meltwater drainage during the early Holocene Epoch, Can. J. Earth Sci., 53,
      321–330, https://doi.org/10.1139/cjes-2015-0135, 2016.

Kemp, A. L. W., Dell, C. I., and Harper, N. S.: Sedimentation Rates and a Sediment Budget for Lake Superior, Journal of
      Great Lakes Research, 4, 276–287, https://doi.org/10.1016/S0380-1330(78)72198-2, 1978.

Lal, D.: Cosmic ray labeling of erosion surfaces: in situ nuclide production rates and erosion models, Earth and Planetary
595   Science Letters, 104, 424–439, https://doi.org/10.1016/0012-821X(91)90220-C, 1991.

Landmesser, C. W., Johnson, T. C., and Wold, R. J.: Seismic Reflection Study of Recessional Moraines beneath Lake
      Superior and Their Relationship to Regional Deglaciation, Quat. res., 17, 173–190, https://doi.org/10.1016/0033-
      5894(82)90057-6, 1982.

Leydet, D. J., Carlson, A. E., Teller, J. T., Breckenridge, A., Barth, A. M., Ullman, D. J., Sinclair, G., Milne, G. A.,
600   Cuzzone, J. K., and Caffee, M. W.: Opening of glacial Lake Agassiz's eastern outlets by the start of the Younger Dryas
      cold period, Geology, 46, 155–158, https://doi.org/10.1130/G39501.1, 2018.

Li, Y.: Determining topographic shielding from digital elevation models for cosmogenic nuclide analysis: a GIS model for
      discrete sample sites, J. Mt. Sci., 15, 939–947, https://doi.org/10.1007/s11629-018-4895-4, 2018.

Lifton, N., Sato, T., and Dunai, T. J.: Scaling in situ cosmogenic nuclide production rates using analytical approximations to
605   atmospheric cosmic-ray fluxes, Earth and Planetary Science Letters, 386, 149–160,
      https://doi.org/10.1016/j.epsl.2013.10.052, 2014.

Loope, H.: Deglacial chronology and glacial stratigraphy of the western Thunder Bay lowland, northwest Ontario, Canada,
      M.S., University of Toledo, Toledo, OH, 91 pp., 2006.

Lowell, T. V., Fisher, T. G., Hajdas, I., Glover, K., Loope, H., and Henry, T.: Radiocarbon deglaciation chronology of the
610   Thunder Bay, Ontario area and implications for ice sheet retreat patterns, Quaternary Science Reviews, 28, 1597–1607,
      https://doi.org/10.1016/j.quascirev.2009.02.025, 2009.

Lowell, T. V., Kelly, M. A., Howley, J. A., Fisher, T. G., Barnett, P. J., Schwart, R., Zimmerman, S. R. H., Norris, N., and
      Malone, A. G. O.: Near-constant retreat rate of a terrestrial margin of the Laurentide Ice Sheet during the last
      deglaciation, Geology, 49, 1511–1515, https://doi.org/10.1130/G49081.1, 2021.

615 Lowell, T. V., Larson, G. J., Hughes, J. D., and Denton, G. H.: Age verification of the Lake Gribben forest bed and the Younger Dryas Advance of the Laurentide Ice Sheet, Can. J. Earth Sci., 36, 383–393, https://doi.org/10.1139/e98-095, 1999.

Lowell, T., Waterson, N., Fisher, T., Loope, H., Glover, K., Comer, G., Hajdas, I., Denton, G., Schaefer, J., Rinterknecht, V., Broecker, W., and Teller, J.: Testing the Lake Agassiz meltwater trigger for the Younger Dryas, Eos Trans. AGU, 86,
620 365, https://doi.org/10.1029/2005EO400001, 2005.

Maher, L. J.: Palynological Studies in the Western Arm of Lake Superior, Quat. res., 7, 14–44, https://doi.org/10.1016/0033-5894(77)90012-6, 1977.

Marrero, S. M., Phillips, F. M., Borchers, B., Lifton, N., Aumer, R., and Balco, G.: Cosmogenic nuclide systematics and the CRONUScalc program, Quaternary Geochronology, 31, 160–187, https://doi.org/10.1016/j.quageo.2015.09.005, 2016.

625 Marshall, S. J., Tarasov, L., Clarke, G. K. C., and Peltier, W. R.: Glaciological reconstruction of the Laurentide Ice Sheet: physical processes and modelling challenges, Can. J. Earth Sci., 37, 769–793, https://doi.org/10.1139/e99-113, 2000.

Mothersill, J. S. and Fung, P. C.: The Stratigraphy, Mineralogy, and Trace Element Concentrations of the Quaternary Sediments of the Northern Lake Superior Basin, Can. J. Earth Sci., 9, 1735–1755, https://doi.org/10.1139/e72-153, 1972.

630 Mothersill, J. S.: Batchawana Bay, Lake Superior: late Quaternary sedimentary fill and paleomagnetic record, Can. J. Earth Sci., 22, 39–52, https://doi.org/10.1139/e85-004, 1985.

Mothersill, J. S.: Paleomagnetic dating of late glacial and postglacial sediments in Lake Superior, Can. J. Earth Sci., 25, 1791–1799, https://doi.org/10.1139/e88-169, 1988.

Mothersill, J. S.: The paleomagnetic record of the late Quaternary sediments of Thunder Bay, Can. J. Earth Sci., 16, 1016–
635 1023, https://doi.org/10.1139/e79-089, 1979.

Nishiizumi, K., Imamura, M., Caffee, M. W., Southon, J. R., Finkel, R. C., and McAninch, J.: Absolute calibration of 10Be AMS standards, Nuclear Instruments and Methods in Physics Research Section B: Beam Interactions with Materials and Atoms, 258, 403–413, https://doi.org/10.1016/j.nimb.2007.01.297, 2007.

Nishiizumi, K., Winterer, E. L., Kohl, C. P., Klein, J., Middleton, R., Lal, D., and Arnold, J. R.: Cosmic ray production rates
640 of 10 Be and 26 Al in quartz from glacially polished rocks, J. Geophys. Res., 94, 17907, https://doi.org/10.1029/JB094iB12p17907, 1989.

O'Beirne, M. D.: Anthropogenic climate change has driven Lake Superior productivity beyond the range of Holocene variability, Ph.D., University of Minnesota, 142 pp., 2013.

Paterson, W. S. B.: Laurentide Ice Sheet: Estimated volumes during Late Wisconsin, Rev. Geophys., 10, 885,
645 https://doi.org/10.1029/RG010i004p00885, 1972.

Peltier, W. R., Argus, D. F., and Drummond, R.: Space geodesy constrains ice age terminal deglaciation: The global ICE-6G_C (VM5a) model: Global Glacial Isostatic Adjustment, J. Geophys. Res. Solid Earth, 120, 450–487, https://doi.org/10.1002/2014JB011176, 2015.

Peterson, R. O.: Wolf ecology and prey relationships on Isle Royale, National Park Service, U.S. Department of the Interior,
650 1977.

Peterson, W. L.: Surficial geologic map of the Iron River 1 degree by 2 degrees Quadrangle, Michigan and Wisconsin, U.S. Geological Survey, https://doi.org/10.3133/i1360C, 1985.

Raymond, R. E., Kapp, R. O., and Janke, R. A.: Postglacial and recent sediments of inland lakes of Isle Royale National Park, Michigan, Michigan Academician, 7, 453–465, 1975.

655 Saarnisto, M.: The Deglaciation History of the Lake Superior Region and its Climatic Implications, Quat. res., 4, 316–339, https://doi.org/10.1016/0033-5894(74)90019-2, 1974.

Schaetzl, R. J., Lepper, K., Thomas, S. E., Grove, L., Treiber, E., Farmer, A., Fillmore, A., Lee, J., Dickerson, B., and Alme, K.: Kame deltas provide evidence for a new glacial lake and suggest early glacial retreat from central Lower Michigan, USA, Geomorphology, 280, 167–178, https://doi.org/10.1016/j.geomorph.2016.11.013, 2017.

660 Stokes, C. R., Margold, M., Clark, C. D., and Tarasov, L.: Ice stream activity scaled to ice sheet volume during Laurentide Ice Sheet deglaciation, Nature, 530, 322–326, https://doi.org/10.1038/nature16947, 2016.

Stone, J. O.: Air pressure and cosmogenic isotope production, J. Geophys. Res., 105, 23753–23759, https://doi.org/10.1029/2000JB900181, 2000.

Stuiver, M. and Reimer, P. J.: Extended 14 C Data Base and Revised CALIB 3.0 14 C Age Calibration Program, Radiocarbon, 35, 215–230, https://doi.org/10.1017/S0033822200013904, 1993.

Tarasov, L., Dyke, A. S., Neal, R. M., and Peltier, W. R.: A data-calibrated distribution of deglacial chronologies for the North American ice complex from glaciological modeling, Earth and Planetary Science Letters, 315–316, 30–40, https://doi.org/10.1016/j.epsl.2011.09.010, 2012.

Teller, J. T. and Mahnic, P.: History of sedimentation in the northwestern Lake Superior basin and its relation to Lake Agassiz overflow, Can. J. Earth Sci., 25, 1660–1673, https://doi.org/10.1139/e88-157, 1988.

Teller, J. T., Boyd, M., Yang, Z., Kor, P. S. G., and Mokhtari Fard, A.: Alternative routing of Lake Agassiz overflow during the Younger Dryas: new dates, paleotopography, and a re-evaluation, Quaternary Science Reviews, 24, 1890–1905, https://doi.org/10.1016/j.quascirev.2005.01.008, 2005.

Teller, J. T., Leverington, D. W., and Mann, J. D.: Freshwater outbursts to the oceans from glacial Lake Agassiz and their role in climate change during the last deglaciation, Quaternary Science Reviews, 21, 879–887, https://doi.org/10.1016/S0277-3791(01)00145-7, 2002.

Teller, J. T.: Volume and Routing of Late-Glacial Runoff from the Southern Laurentide Ice Sheet, Quat. res., 34, 12–23, https://doi.org/10.1016/0033-5894(90)90069-W, 1990.

Thomas, R. L. and Dell, C. I.: Sediments of Lake Superior, Journal of Great Lakes Research, 4, 264–275, https://doi.org/10.1016/S0380-1330(78)72197-0, 1978.

Ullman, D. J., Carlson, A. E., LeGrande, A. N., Anslow, F. S., Moore, A. K., Caffee, M., Syverson, K. M., and Licciardi, J. M.: Southern Laurentide ice-sheet retreat synchronous with rising boreal summer insolation, Geology, 43, 23–26, https://doi.org/10.1130/G36179.1, 2015.

Yu, S.-Y., Colman, S. M., Lowell, T. V., Milne, G. A., Fisher, T. G., Breckenridge, A., Boyd, M., and Teller, J. T.: Freshwater Outburst from Lake Superior as a Trigger for the Cold Event 9300 Years Ago, Science, 328, 1262–1266, https://doi.org/10.1126/science.1187860, 2010.